Vol. 02, Iss. 4 (2025) 197-204, DOI: 10.61552/JSI.2025.04.003

JSDI

Journal of Sustainable Development Innovations

www.jsi.aspur.rs

High Gain Dual-Polarization Antenna at 2.4 GHz Wi-Fi Applications

Ahmed A. Salih[a], Abdulkareem S. Abdullah[b,*]

[a]*Biomedical Engineering Department, College of Engineering, University of Thi-Qar, Nassiriya, Iraq,*
[b]*Department of Electrical Engineering, College of Engineering, University of Basrah, Basrah, Iraq.*

Keywords:

Dual-polarization antenna, Microstrip patch antennas, Wireless local area network, Wi-Fi Application, aperture-coupled feed, and capacitive-coupled feed.

* Corresponding author:

Abdulkareem S. Abdullah
E-mail:
abdulkareem.abdullah@uobasrah.edu.iq

Received: 1 November 2024
Revised: 12 December 2024
Accepted: 27 January 2025

A B S T R A C T

In this paper, a high-gain dual-polarization antenna of size (100×100) mm² has been designed and analyzed to work at 2.4 GHz for Wi-Fi applications. The adopted antenna is of rectangular shape, which is fed from two ports to provide a dual-polarization operation and increase the possibility of getting the RF signal. The dual-polarization operation is achieved by coupling two different feeds to the rectangular patch at the required resonant frequency of 2.4 GHz. The first feed is an aperture-coupled feed and the second is a capacitive-coupled feed. The simulated reflection coefficients of the two ports are found as S_{11} = -18.4887 dB and S_{22} = -22.6915 dB at 2.4 GHz. A very high isolation of S_{12} = - 63 dB and S_{21} = - 60.67 dB are also achieved at the designed frequency of 2.4 GHz. The achieved bandwidths for port-1 and port-2 are found as 191.33 MHz (a percentage value of 7.97%) and 264.06 MHz (a percentage value of 11%) respectively. The maximum gain values of the two ports are found as 8.11 dB and 7.42 dB respectively.

1. INTRODUCTION

A wireless local area network (WLAN) is a wireless computer network that connects multiple devices utilizing a wireless distribution mechanism, within a confined area such as a residence, educational institution, computer facility, or commercial structure. This feature enables users to navigate inside a specific geographical area while maintaining connectivity to the network, and can also establish a link to the broader Internet. Wireless LANs have gained popularity in residential settings due to their simple installation and user-friendly nature [1]. They are also commonly found in commercial complexes that provide wireless access to their customers. The list of WLAN channels refers to the authorized set of wireless local area network channels that comply with IEEE 802.11 protocols. The 802.11 workgroup presently records usage at four separate frequency ranges: 2.4 GHz, 3.6 GHz, 4.9 GHz, 5 GHz, and 5.9 GHz bands [2]. The range is subdivided into numerous channels, and each country enforces its own restrictions regarding the permissible frequency ranges, authorized users, and maximum power levels for these channels. Amateur Radio operators, who are licensed in certain nations, including the United States, are allowed to utilize specific channels with significantly increased power levels for long-range wireless communication [3].

The antenna is an essential component in wireless application systems. Microstrip antennas (MSA) exhibit versatility in terms of their geometric configurations and applications [4].

MSA can be used in wireless applications due to its characteristics such as ease of installation, lightweight, and ease of mass production. Although many properties make the microstrip antenna well-suited for deployment in wireless applications, there is a very serious limitation which is the narrow bandwidth. Typical bandwidth of microstrip antennas is between 1% and 3% [5]. The full potential of the microstrip antenna can be realized by overcoming this constraint. To increase the bandwidth of the microstrip antenna, different methods of bandwidth improvement are investigated and suggested. The bandwidth and gain of most wireless communication systems are not met by the microstrip antenna in its most basic configuration [6]. A novel microstrip antenna construction for wireless applications has been investigated to create an affordable, effective patch antenna for both indoor and outdoor applications. The suggested design can be used as an external antenna for routers, modems, switches, and other equipment, or it can be used indoors for portable electronics like laptops, smartphones, and mobile phones. The signals are not only propagating in a direct line of sight [7], but maybe dispersed, diffused, and reflected. As a result, signals typically arrive at their destination via multiple paths. The signal tends to cancel each other if they travel on different paths and arrive at the destination 90 degrees out of phase and a decrease in the antenna performance would occur. The multipath effect is encountered in dual polarization antenna since two different polarization signals can originate from it [8]. These signals then arrive at the same location as two separate signals. Thus, they won't be able to recognize one another, and the signal won't be canceled. In addition, polarization diversity is crucial for improving system performance and lowering interference and the multipath effect. Moreover, an antenna with dual polarization can boost the effective channel capacity. This is because dual polarization antennas allow for communication with several systems while consuming the same amount of bandwidth and transmit power [9]. The emerging new technologies resulted in an even greater congestion of the frequency bands used by various wireless protocols. To handle the increased demands brought on by this growth, dependable communications systems have had to advance at the same quick speed. To push systems capabilities beyond what has previously been possible, new technologies and methodologies must be developed [10]. This presents new challenges in the form of designing wideband antennas to overcome the majority of microstrip antenna defects and to keep up with the growing demand for more data processing.

2. ANTENNA DESIGN

In this paper, the adopted antenna is of rectangular shape patch that is fed from two ports to provide a dual-polarization operation and increase the possibility of getting the RF signal. The dual-polarization operation is achieved by arranging two different feeds, which are coupled to the rectangular patch as shown in Fig.1. The first feed is an aperture-coupled feed and the second one is a capacitive-coupled feed and is used to obtain the required resonant frequency of 2.4 GHz. FR4 is chosen as the substrate to design this antenna with specifications as listed in Table 1.

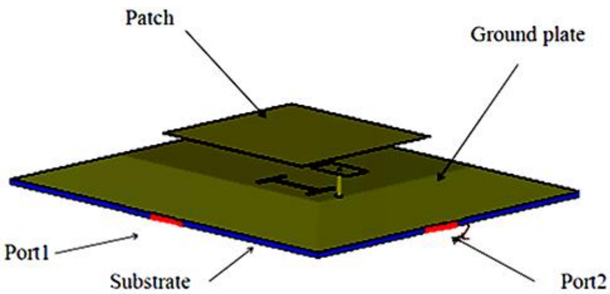

Fig. 1. Dual-polarized stack microstrip Antenna.

Table 1. The specifications of the dielectric substrate [11].

Dielectric material	CEM-1(loss-free) FR4
Dielectric constant ε_r	4.4
Substrate height (h)	1.6 mm
Loss tangent	0.004

2.1 Design of the Rectangular Patch

The design of the rectangular patch can be achieved by applying the classical formulae and commences with choosing the patch with (W) as [12-15]:

$$W = \frac{1}{2f_r\sqrt{\varepsilon_\circ\mu_\circ}}\sqrt{2/(\varepsilon_r + 1)} \quad (1)$$

where,

f_r - the resonant frequency.

ε_0 - the absolute permittivity of free space.

μ_0 - the absolute permeability of free space.

ε_r - the dielectric constant of the substrate.

The effective permittivity ε_{reff} of the dielectric substrate is calculated by:

$$\varepsilon_{reff} = \frac{\varepsilon_r + 1}{2} + \frac{\varepsilon_r - 1}{2\sqrt{1 + 12\,h/W}} \quad (2)$$

where (h) is the thickness of the dielectric substrate. The line extension (ΔL) due to fringing is computed by :

$$\Delta L = \frac{0.412h(\varepsilon_{reff} + 0.3)(\,W/h + 0.264)}{[(\varepsilon_{reff} - 0.258)(W/h + 0.8)]} \quad (3)$$

The length (L) of the patch is obtained by applying the following equation:

$$L = \frac{1}{2f_r\sqrt{\varepsilon_{reff}}\sqrt{\varepsilon_0\mu_0}} - 2\Delta L \quad (4)$$

The original computed values of (W) and (L) necessary to resonate the antenna at 2.4 GHz are found as 38 mm and 41.02 mm respectively using Eq. (1) to Eq. (4). It is worth mentioning that after adding the H-slot and capacitor in the next two sections of this paper, the resonant frequency is shifted slightly from 2.4 GHz. Therefore a parametric study is done to adapt the patch width and length to restore a resonance of 2.4 GHz. The modified values of (W) and (L) are found as 45.4 mm and 49.035 mm respectively.

2.2 Design of Aperture–Coupled Feed

The first feed is an aperture-coupled feed, which has the shape of an H-slot cut in the ground plane as shown in Fig.2. It is used to couple the electromagnetic energy from the 50 Ω microstrip feed line printed on the other side of the substrate. The microstrip feed line has a width of 4.5 mm, which is necessary to give 50 Ω characteristics impedance. The equivalent circuit of the antenna with the H-slot is shown in Fig.3.

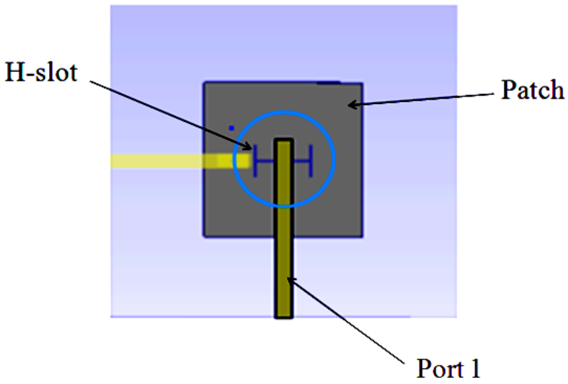

Fig. 2. H-slot coupled.

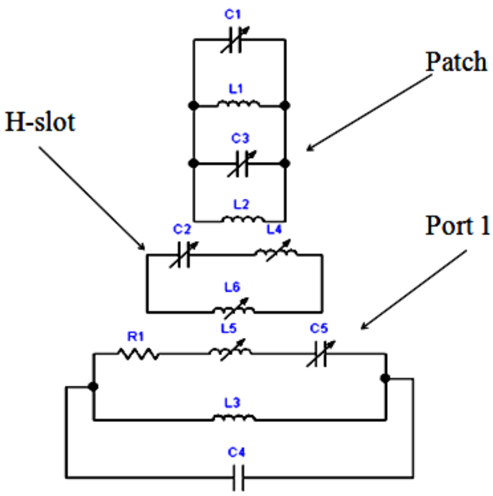

Fig. 3. Equivalent circuit of the antenna with H-slot [16-17].

The slot width of the H-shaped slot is taken as 1 mm, which allows efficient electromagnetic energy coupling and reduction of the back radiation of the slot. The length of the slot central arm and the two side arms are designated as H. The optimum dimensions of H and the length of the microstrip feed line are obtained via parametric studies so that the antenna reflection coefficient has a small value and a good impedance matching over a wide frequency range can be achieved for this antenna. The variation of the slot central arm length with frequency is shown in Fig.4. It is found that a value of 20 mm gives the lowest value of antenna reflection coefficient at 2.4 GHz.

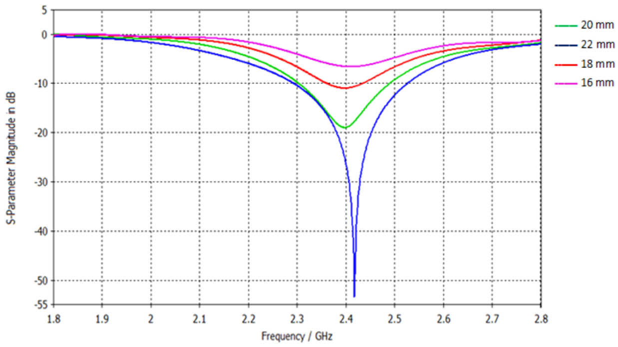

Fig. 4. Variation of slot central arm length with the frequency.

The variation of the slot side arm with frequency is shown in Fig.5. It is found that a value of 19 mm gives the lowest value of antenna reflection coefficient at 2.4 GHz.

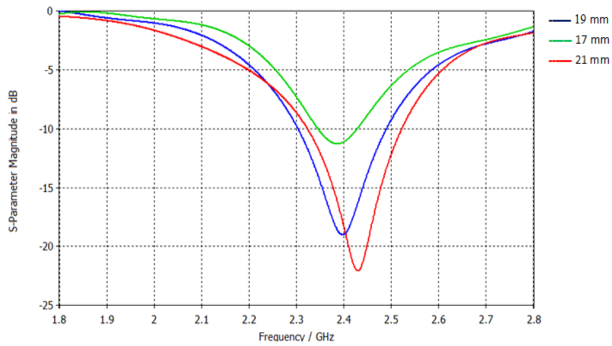

Fig. 5. Variation of slot side arm length H with the frequency.

The variation of microstrip feed line length with frequency is shown in Fig.6. It is found that a length value of 57 mm is necessary to give the lowest reflection coefficient at 2.4 GHz.

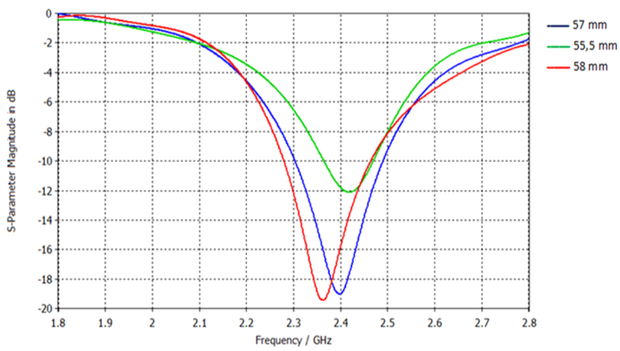

Fig. 6. Variation of microstrip feed line length with the frequency.

2.3 Design of Capacitive-Coupled Feed

The second feed is a capacitive-coupled feed, which has the shape of an L-strip as shown in Fig.7. It consists of a 50 Ω microstrip feed line and a conducting plate that is placed parallel and below the radiating patch at a distance of (g). The conducting plate couples the electromagnetic energy to the radiating patch from the 50 Ω microstrip feed line through a hole in the ground plane. The conducting plate is supported by a conducting post with a height of (d). The equivalent circuit of the antenna with this feed is shown in Fig.8.

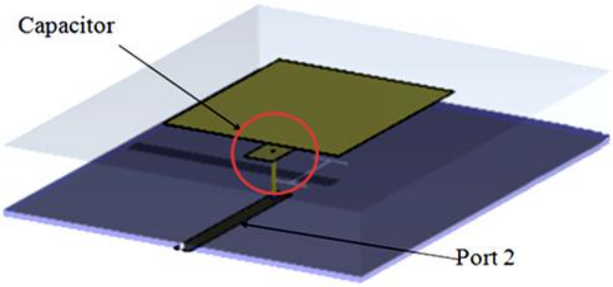

Fig. 7. Capacitive-coupled feed.

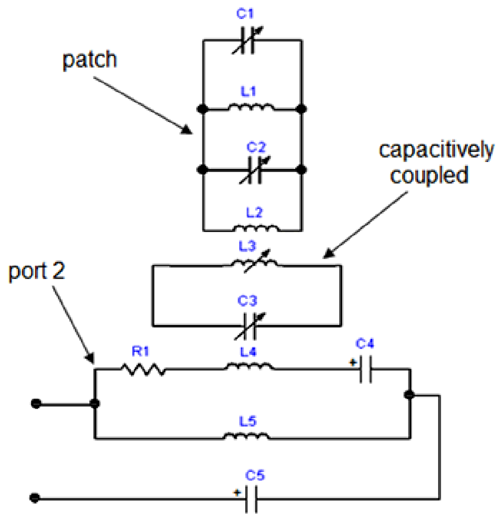

Fig. 8. Equivalent circuit of the antenna with capacitive-coupled feed [18-19].

The optimum dimensions of the conducting plate and the gap between it and the radiating patch are obtained via parametric study so that the antenna has minimum reflection coefficient value and good impedance matching at the designed frequency. The variation of the conducting plate length with frequency is shown in Fig.9. It is found that a value of 10 mm is necessary to obtain the minimum value of the reflection coefficient at 2.4 GHz.

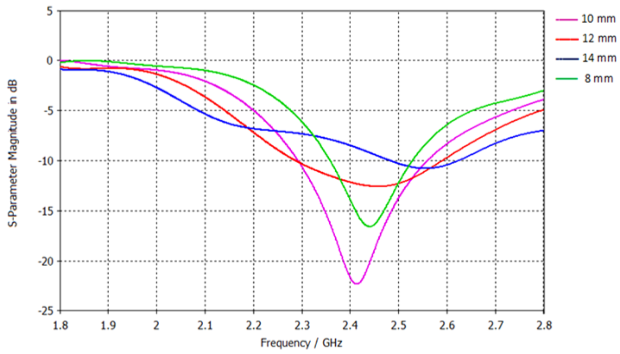

Fig. 9. Variation of conducting plate length with the frequency.

The variation of the conducting plate width with frequency is shown in Fig.10. It is found that a value of 4 mm is required to obtain the lowest value of the reflection coefficient at 2.4 GHz.

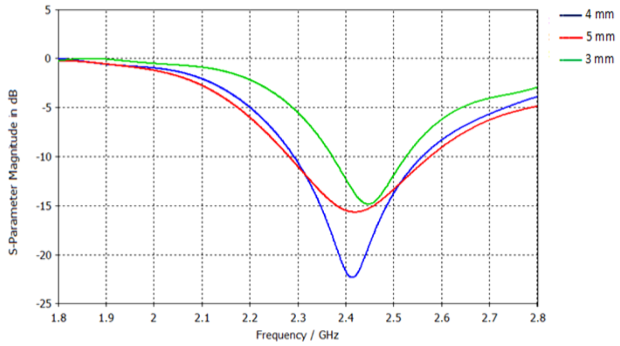

Fig. 10. Variation of conducting plate width with the frequency.

The variation of gap length between the radiating plate and conducting plate is shown in Fig.11. An optimum value of 0.4 mm is necessary to produce the minimum value of the reflection coefficient at 2.4 GHz.

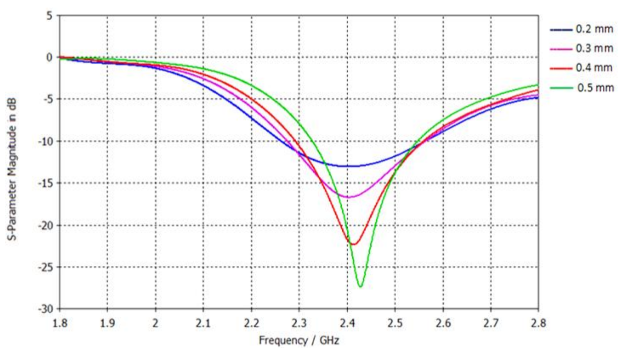

Fig. 11. Variation of gap length between the patch and conducting plate with the frequency.

The final optimum dimensions of the dual-polarized stack microstrip antenna are tabulated in Table -2.

Table 2. The optimum dimensions of the dual-polarized.

Element	Dimensions
Ground plan size	100×100 mm^2
Substrate size	100×100 mm^2
Radiating patch	L=49.035mm ,W=45.4mm
Conductor thickness	0.035 mm(Copper)
H-Slot dimensions	Center-arm=1 × 20 mm^2 Side-arm=1 × 19 mm^2
Port-1	4.5 × 57 mm^2
Port-2	4.5 × 40 mm^2
Plate	L=10 mm , W=4 mm , gap=0.4 mm

3. SIMULATION RESULTS OF THE DUAL-POLARIZED STACK MICROSTRIP ANTENNA

3.1 VSWR

Fig.12 shows the variation of the VSWR values with frequency for the two ports of the dual-polarized stack microstrip antenna. At 2.4 GHz, VSWR values of 1.4287 and 1.1583 are obtained for port-1 and port-2 respectively.

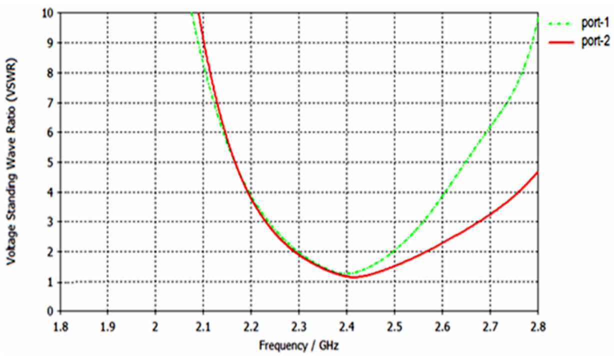

Fig. 12. Variation of VSWR values with frequency for the two ports of the dual-polarized stack microstrip antenna.

3.2 Reflection Coefficient

Fig.13 shows the reflection coefficients (S_{11} , S_{22}) and the isolations (S_{12} , S_{21}) with frequency for the two ports of the dual-polarized stack microstrip antenna. It is clear that a reasonable value of S_{11} = -18.4887 dB and S_{22} = -22.6915 dB are obtained at the required frequency of 2.4 GHz. It is also obvious that very high isolations of S_{12} = - 63 dB and S_{21} = - 60.67 dB are achieved at the designed frequency of 2.4 GHz. Therefore, the power crossed from one port to another is very low.

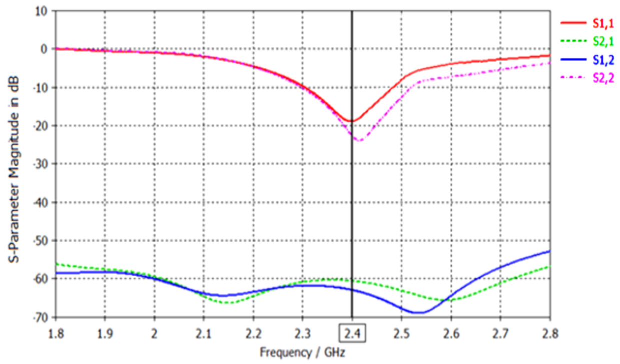

Fig. 13. Reflection coefficients and isolation with frequency for the two ports of the dual-polarized stack microstrip antenna.

3.3 Bandwidth

The dual-polarized stack microstrip antenna bandwidth for port-1 is calculated from Fig.14 as 191.33 MHz, which constitutes a percentage value of 7.9%. From Fig.15, the bandwidth for port-2 is found as 264.06 MHz, which constitutes a percentage value of 11%. Both bandwidth values are as large as compared with that of a simple patch antenna.

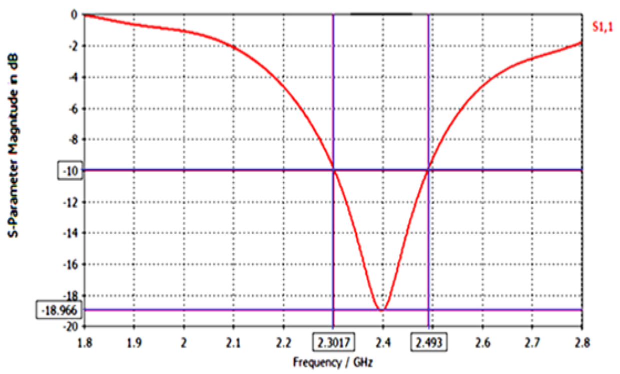

Fig. 14. Bandwith calculation for port-1 of the dual-polarized stack microstrip antenna.

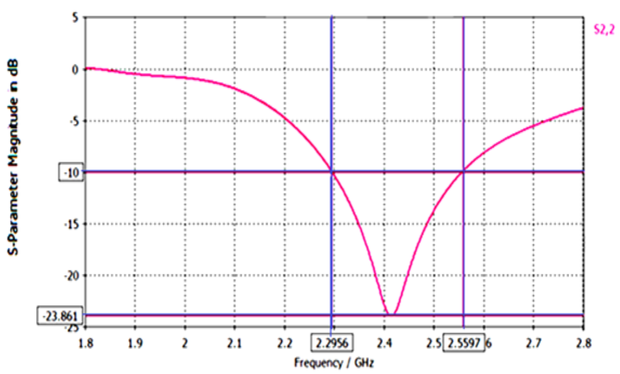

Fig. 15. Bandwith calculation for port-2 of the dual-polarized stack microstrip antenna.

3.4 Radiation pattern

For port-1

The E-plane radiation pattern of the antenna for port-1 excitation is taken at $\Phi = 90^0$ (YZ plane) as shown in Fig.16a. The main lobe direction and HPBW are found as 0^0 and 59.3^0 respectively. The side-lobe level is found as -12.8 dB. The H-plane radiation pattern for this port is shown in Fig.16b.

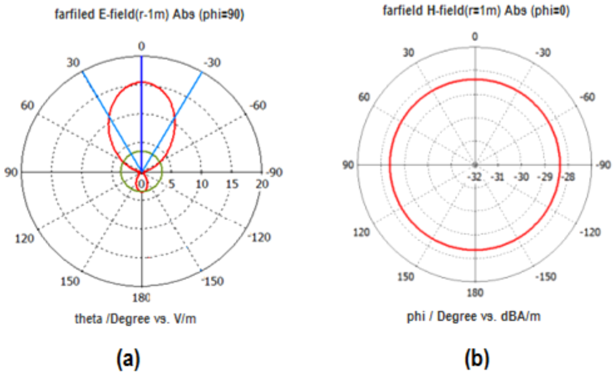

Fig. 16. Radiation pattern for port-1 of the dual-polarized stack microstrip antenna.
a- E-palne b- H-plane

The 3D radiation pattern of this antenna for port-1 is shown in Fig.17.

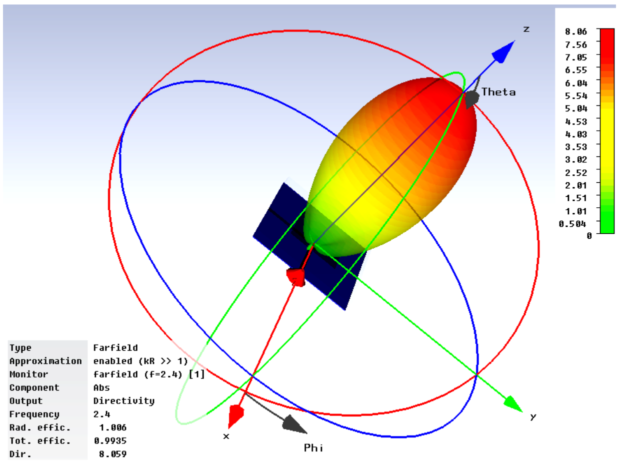

Fig. 17. The 3D radiation pattern for port-1 of the dual-polarized stack microstrip antenna

For port-2

The E-plane radiation pattern of the antenna for port-2 excitation is taken at $\Phi = 0^0$ (XZ plane) as shown in Fig.18a.The main lobe direction and HPBW are found as 9^0 and 62.6^0 respectively. The side-lobe level is found as -16.9 dB. The H-plane radiation pattern for this port is shown in Fig.18b.

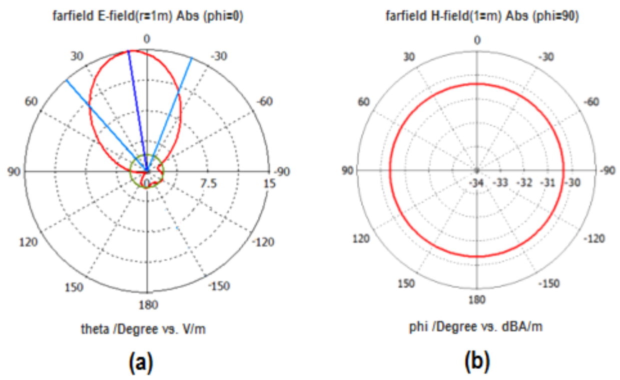

Fig. 18. Radiation pattern for port-2 of the dual-polarized stack microstrip antenna.
a- E-palne b- H-plane

The 3D radiation pattern of this antenna for port-2 is shown in Fig. 19.

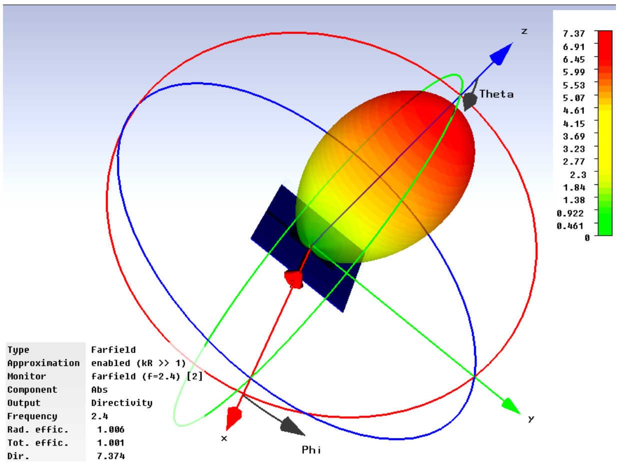

Fig. 19. The 3D radiation pattern for port-2 of the dual-polarized stack microstrip antenna.

3.5 Gain

The variation of gain values with frequency for port-1 and port-2 are shown in Fig.20 and Fig.21 respectively. Values of 8.11 dB and 7.42 dB are obtained for the consecutive ports.

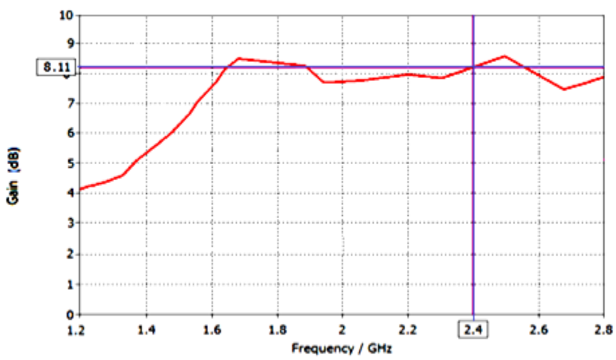

Fig. 20. Variation of gain with frequency for port-1 of the dual-polarized stack microstrip antenna.

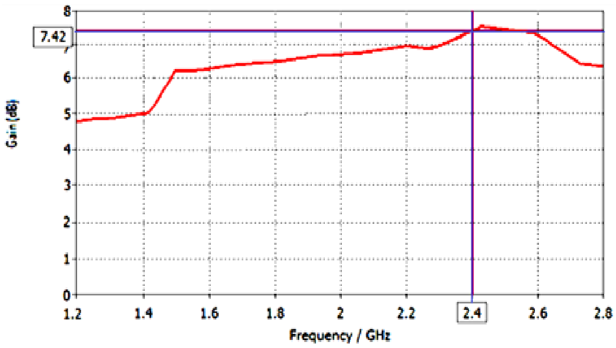

Fig. 21. Variation of gain with frequency for port-2 of the dual-polarized stack microstrip antenna.

4. CONCLUSION

Microstrip antennas are very popular now because they have the advantage of meeting the demand for small, lightweight, compatible, and easy-to-integrate antennas. An antenna is designed and simulated in this paper at 2.4 GHz for Wi-Fi applications with good features of high gain and dual polarization. FR4 is chosen as the substrate with a dielectric constant of ε_r = 4.4, loss tangent of 0.004, and thickness h = 1.6 mm. Simulation results show good reflection coefficient values of S_{11} = -18.4887 dB and S_{22} = -22.6915 dB for the two ports. It is also obvious that very high isolation values between the two ports of S_{12} = - 63 dB and S_{21} = - 60.67 dB are achieved at the designed frequency of 2.4 GHz. High gain values of 8.11 dB and 7.42 dB are obtained for the consecutive ports.

REFERENCES

[1] A. Singh, A. Vaish, and P. Keserwani, "Research Issues and Challenges of Wireless Networks," *International Journal of Advanced Research in Computer Science and Software Engineering*, vol. 4, no. 2, pp. 572–575, 2014.

[2] IEEE, "802.11-1999 - IEEE Standard for Information Technology - Telecommunications and Information Exchange Between Systems - Local and Metropolitan Area Networks - Specific Requirements - Part 11: Wireless LAN Medium Access Control (MAC) and Physical Layer (PHY) Specifications," 31 Dec. 2003, doi: 10.1109/IEEESTD.2003.95617.

[3] Y. K. Park and Y. Sung, "A reconfigurable antenna for quad-band mobile handset applications," *IEEE Transactions on Antennas and Propagation*, vol. 60, no. 6, pp. 3003–3006, 2012, doi: 10.1109/TAP.2012.2194672.

[4] A. A. Salih and M. Nangir, "Design and Analysis of Wireless Power Transmission (2X1) MIMO Antenna at 5G-Frequencies for Applications of Rectenna Circuits in Biomedical," *Journal of Wireless Mobile Networks, Ubiquitous Computing, and Dependable Applications (JoWUA)*, vol. 15, no. 3, pp. 203–221, 2024, doi: 10.58346/JOWUA.2024.I3.014.

[5] N. K. Reddy, A. Hazra, and V. Sukhadeve, "A compact elliptical microstrip patch antenna for future 5G mobile wireless communication," *International Journal of Advanced Engineering and Management*, vol. 2, no. 7, pp. 153–156, 2017, doi: 10.24999/IJOAEM/02070036.

[6] A. S. Dhillon, D. Mittal, and E. Sidhu, "THz rectangular microstrip patch antenna employing polyimide substrate for video-rate imaging and homeland defense applications," *Optik*, vol. 144, pp. 634–641, 2017, doi: 10.1016/j.ijleo.2017.07.018.

[7] R. Mishra, J. Jayasinghe, R. G. Mishra, and P. Kuchhal, "Design and Performance Analysis of a Rectangular Microstrip Line Feed Ultra-Wide Band Antenna," *International Journal of Signal Processing, Image Processing and Pattern Recognition*, vol. 9, no. 6, pp. 419–426, 2016, doi: 10.14257/ijsip.2016.9.6.36.

[8] S. J. Yang, R. Ma, and X. Y. Zhang, "Self-decoupled dual-band dual-polarized aperture-shared antenna array," *IEEE Transactions on Antennas and Propagation*, vol. 70, no. 6, pp. 4890–4895, 2022, doi: 10.1109/TAP.2021.3137531.

[9] Nasimuddin and X. Qing, "A Miniaturized Wideband Circularly Polarized Antenna Using Metasurface," in *16th European Conference on Antennas and Propagation (EuCAP)*, Madrid, Spain, pp. 1–5, Mar. 27–Apr. 1, 2022, doi: 10.23919/EuCAP53622.2022.9768941.

[10] H. Wong, K. L. Lau, and K. M. Luk, "Design of dual-polarized L-probe patch antenna arrays with high isolation," *IEEE Transactions on Antennas and Propagation*, vol. 52, no. 1, pp. 45–52, 2004, doi: 10.1109/TAP.2003.822402.

[11] W. A. Neamah, A. A. Salih, N. J. Aklo, and M. Nangir, "Design of three selectable notched bands UWB antenna for wireless application," in *AIP Conference Proceedings*, vol. 2845, p. 050014, AIP Publishing, 2023, doi: 10.1063/5.0157611.

[12] C. A. Balanis, *Antenna Theory - Analysis and Design*, 4th ed., Wiley-Interscience, 2012.

[13] A. A. Salih, M. Nangir, W. A. Neamah, and S. H. Hassan, "Design a compact UWB antenna for breast tumor detection system," in *AIP Conference Proceedings*, vol. 2845, p. 030001, AIP Publishing, 2023, doi: 10.1063/5.0170497.

[14] S. Ashraf, J. A. Sheikh, A. Ashraf, and U. Rasool, "Comparative analysis of rectangular framed S-shaped millimeter-wave antenna for different feeding techniques," *Materials Today: Proceedings*, vol. 74, Part 2, pp. 123–129, 2023, doi: 10.1016/j.matpr.2022.08.029.

[15] A. A. Salih and A. S. Abdullah, "Design and analysis of a compact dual-band printed rectenna circuit at WiFi and GSM frequencies for microwave power transmission," in *AIP Conference Proceedings*, vol. 2591, p. 030023, AIP Publishing, 2023, doi: 10.1063/5.0129460.

[16] M. Narayanan, G. Ramkumar, and G. Anitha, "Enhanced RF Characteristics of Frequency Reconfigurable Microstrip Patch Antenna using Aperture-Coupled Feeding at 5 GHz," in *2024 4th Asian Conference on Innovation in Technology (ASIANCON)*, India, pp. 1–5, 2024, doi: 10.1109/ASIANCON62057.2024.10838107.

[17] W. A. Neamah, H. M. Al Sabbagh, and H. Al-Rizzo, "New Design of a Compact 1×2 Super UWB-MIMO Antenna for Polarization Diversity," *Iraqi Journal For Electrical and Electronics Engineering*, vol. 19, no. 1, 2023, doi: 10.37917/ijeee.19.1.14.

[18] J. H. Jun, B. J. Kim, S. K. Shin, K. Jang, J. S. Baek, and C. Kim, "In-cell self-capacitive-type mobile touch system and embedded readout circuit in display driver IC," *Journal of Display Technology*, vol. 12, no. 12, pp. 1613–1622, 2016, doi: 10.1109/JDT.2016.2624300.

[19] Y. Zhang and Y. Zhang, "Dual-band dual-polarized antenna using a simple radiation restoration and decoupling structure," *IEEE Antennas and Wireless Propagation Letters*, vol. 22, no. 4, pp. 709–713, 2022, doi: 10.1109/LAWP.2022.3222863.